

## **Direct observation of stepwise movement of a synthetic molecular transporter.**

Shelley Wickham, Masayuki Endo, Yousuke Katsuda, Kumi Hidaka, Jonathan Bath,  
Hiroshi Sugiyama, and Andrew J Turberfield

**This file includes:****1. Supplementary Methods****2. Supplementary Figures**

- Supplementary Fig. 1. Origami track design, AFM experiments .
- Supplementary Fig. 2. Origami track design, fluorescence experiments.
- Supplementary Fig. 3. Ion-exchange HPLC.
- Supplementary Fig. 4. Origami tile repair.
- Supplementary Fig. 5. Kinetic model for stepping rate analysis.
- Supplementary Fig. 6. Rate dependence on temperature and buffer conditions.
- Supplementary Fig. 7. Fluorescence experiment, stepping along broken tracks.
- Supplementary Fig. 8. Fluorescence experiment, intermolecular transfer on split tile.
- Supplementary Fig. 9. Rate of motor transport between tiles in solution.
- Supplementary Fig. 10. Rate of motor diffusion along a track.
- Supplementary Fig. 11. Broken track AFM experiment, no S<sub>7</sub>.
- Supplementary Fig. 12. Kymograph for Supplementary Movie 2 .
- Supplementary Fig. 13. Kymographs for additional AFM movie data .
- Supplementary Fig. 14. Kymograph, hairpin controls.
- Supplementary Fig. 15. Height profile data for AFM movies.

**3. Supplementary Table**

- Supplementary Table 1. DNA sequences for modified staple strands.
- Supplementary Table 2. DNA sequences for unmodified staples, origami type B.

**4. Supplementary Movies**

- Supplementary Movie 1. Two-step movie.
- Supplementary Movie 2. One-step movie.

**5. Supplementary Notes**

## 1. Supplementary Methods

**Origami design.** Two designs were used for the DNA origami rectangle. Tile type A was used for AFM experiments, and consists of a uniform set of 216 32-nt staples, taken directly from a previously published design<sup>1</sup>. This gives a rectangular tile of 288 basepair (bp) helices crosslinked at 16 bp intervals. Such designs have a global right-handed twist as a result of slight underwinding (10.7 bp/turn) of the DNA helices between crossover positions<sup>2</sup>. Tile Type B is a modification of Type A, designed to reduce global twist. Six nucleotides of the template strand are skipped along each of the 24 helices, such that the skipped bases are evenly distributed across the tile. The resulting tile consists of 72 32-nt staples and 144 31-nt staples, as listed in Supplementary Table 2. Tile type B has 282 bp helices cross-linked on average every 15.6 bp, with a more optimal average value of 10.4 bp/turn.

**Origami synthesis.** Single-stranded M13mp18 DNA was ordered from USB (Affymetrix) as the template strand for the origami rectangle. Staple strands were purchased from Integrated DNA Technologies (IDT). Unmodified staples were purchased unpurified. Stator-modified staples were purchased PAGE-purified. Fluorescently labeled strands F<sub>1</sub> (JOE), F<sub>2</sub> (Cy5) and motor (IowaBlackRQ) were purchased HPLC-purified. The fluorescently labeled staples F<sub>3</sub> (Cy3.5), F<sub>4</sub> (Cy3.5) and F<sub>8</sub> (Cy3.5) were purchased unpurified with 3' amine modification and conjugated to Cy3.5 NHS ester dye (GE Healthcare) following manufacturers instructions, then purified by reverse-phase HPLC (Waters). The solution for origami synthesis contained 50 nM M13mp18, 250 nM of each staple strand (5-fold excess), 1× tris-acetate buffer with 12.5 mM magnesium acetate (pH 8.3). The resulting solution was annealed from 95 °C to 20 °C in a PCR machine at an average rate of 1 °C/minute in 0.1 °C steps.

**Tile repair.** Origami tiles annealed with all but one of the staple strands were incubated with the missing staple following different protocols, and the insertion efficiency was quantified (Supplementary Fig. 4). On the basis of these results, incubation conditions used in fluorescence experiments to load the motor at the start of the track were chosen: 1 hour, at 37 °C, with a 0.9× excess of the S<sub>1</sub> + motor duplex. The S<sub>1</sub> + motor duplex

was pre-annealed by combining the stator S<sub>1</sub> and motor at ratio 1:0.95, heating to 95 °C, and cooling to 20 °C in a PCR machine at a rate of 7.5 °C/minute.

**Origami purification.** Excess staples were separated from the origami by gel filtration through hand-packed columns using Sephadryl S-300 HR (GE Healthcare). This is a size-exclusion resin with DNA exclusion limit of 118 bp. Origami samples of up to 60 μL were purified 3 times, on columns of ~500 μL resin volume, by centrifugation at 1000 g for 4 minutes. This gave a low background level for fluorescence measurements with only a small loss in sample.

**Enzyme.** Nicking enzyme Nt.BbvCI was purchased from New England Biolabs and added to the purified origami samples, such that the final solution contained 10 units of enzyme in 1× tris-acetate buffer with 12.5 mM magnesium acetate and 50 mM NaCl (pH 8.3), in a final volume of 140 μL.

**Gel electrophoresis.** DNA origami were run on 0.75% agarose gels in 1 × TAE buffer at 80 V for 2 hours at 4 °C. Gels were scanned with a BioRad PharosFX Plus gel scanner. Gels with fluorescent staple strands were pre-scanned with a 532 nm/605 nm excitation/emission filter pair. All gels were stained with SyBr Gold (Invitrogen) nucleic acid gel stain, and scanned at Ex/Em 488 nm/530 nm.

**HPLC.** The efficiency of strand inclusion was quantified by HPLC with an ion exchange column (DEAE Sepharose, GE Healthcare), which traps DNA at low salt concentrations (100mM NaCl, 1×tris-acetate, 12.5 mM magnesium acetate). The DNA is eluted with an increasing NaCl gradient, separating the origami from the staple strands. A sample trace and agarose gel of the peaks detected is shown in Supplementary Fig. 3. The absorbance of the eluent at 260 nm was used to detect DNA, and fluorescence (Ex/Em 529 nm/555 nm) was used to determine the amount of a single fluorescent staple strand inserted into the tiles. The area of the fluorescence peak for the labeled origami was normalized by the area of the corresponding DNA absorbance peak to allow comparison of insertion efficiencies for different samples.

**Fluorescence measurements.** Fluorescence of origami track samples was measured as a function of time in a Cary Eclipse Fluorescence Spectrometer (Varian) in 100 μL

quartz cuvettes (Starna). Mineral oil (Sigma) was added to cuvettes to prevent evaporation. Excitation and emission wavelengths were as follows: Cy3 (545 nm/565 nm), Cy5 (645 nm/665 nm), Cy3.5 (575 nm/595 nm), JOE (529 nm/555 nm). Slit widths were 5 nm (excitation) and 10 nm (emission). Fluorescence intensities were measured every 10 s, with an integration time of 1 s. Sample concentrations used were in the range 15 nM – 25 nM. Initial fluorescence signals (100%) and the signals in the presence of excess motor (0%) were used to set the base line and to normalize signals from different fluorophores.

**AFM experiments.** A sample solution (50 µL) containing 10 nM M13mp18 single-stranded DNA (New England Biolabs), 50 nM staple DNA strands (5 eq), 20 mM Tris-HCl (pH 7.6), 1 mM EDTA, and 10 mM MgCl<sub>2</sub> was annealed from 85 °C to 15 °C at a rate of 1.0 °C/min, using a thermal cycler. Origami tiles were gel-purified, as described above. The S<sub>1</sub>-motor duplex (5 eq) was incubated with the DNA tiles at 23 °C. Prepared samples were treated with 20 units of restriction enzyme Nt.BbvCI (New England Biolabs) in a 20 µL solution containing 20 mM Tris-HCl (pH 7.6), 1 mM EDTA and 10 mM MgCl<sub>2</sub> and incubated at 23°C for 0, 1, 2, and 3 hours. Histograms of the distribution of motor over stators were averaged over 3 independent trials with N<sub>1</sub>= (28, 53, 41, 53), N<sub>2</sub>= (40, 44, 46, 41), N<sub>3</sub>= (41, 42, 39, 41) tiles counted for the 4 time steps in each trial respectively.

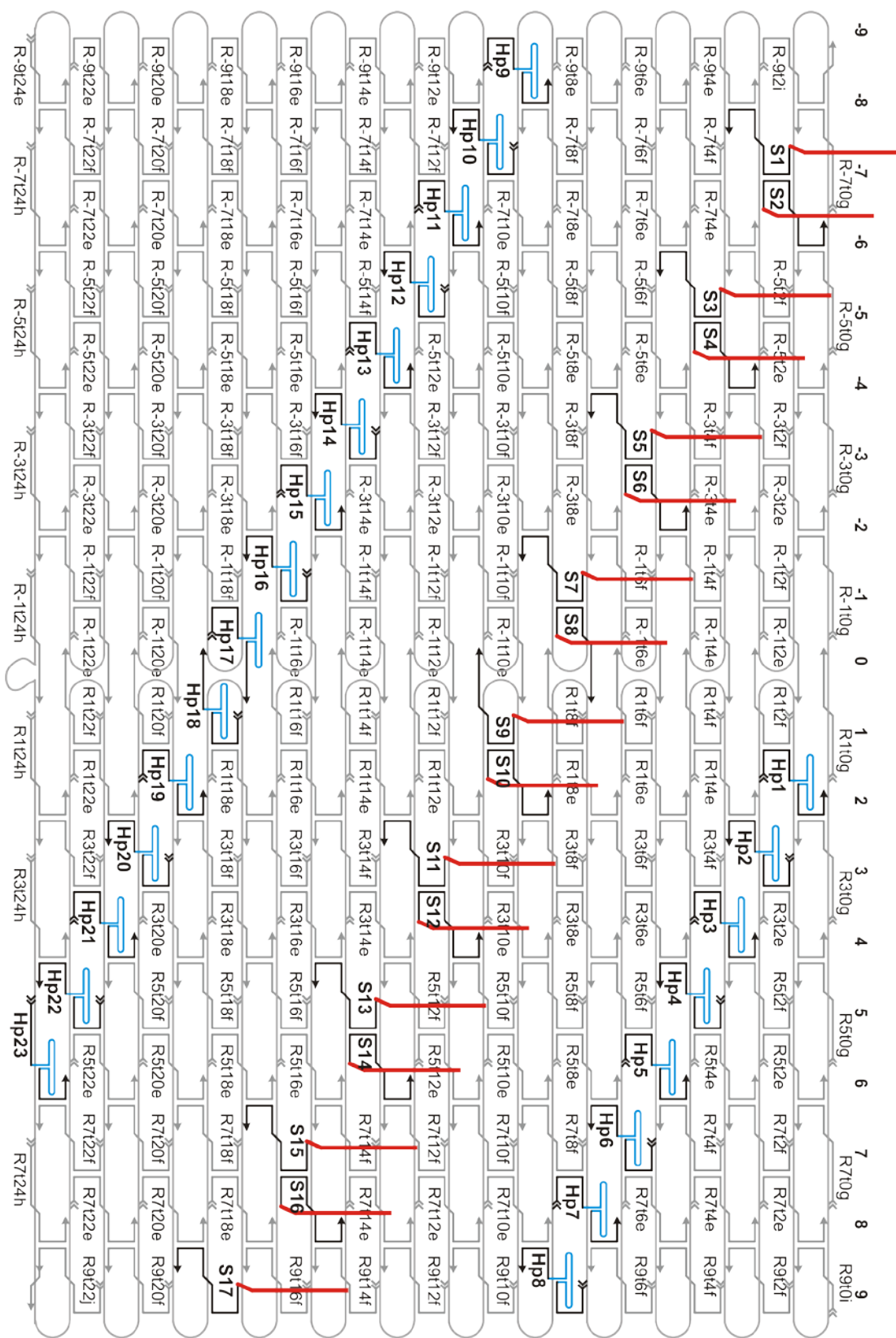
**High-speed AFM imaging.** AFM images were obtained using a high-speed AFM imaging system (Nano Live Vision, RIBM, Tsukuba, Japan) with a silicon nitride cantilever (Olympus BL-AC10EGS). Samples (2 µL) were adsorbed onto a freshly cleaved mica surface for 5 min at room temperature and then washed three times using the buffer solution used for sample preparation. Scanning was performed at 23 °C in the same buffer solution using a tapping mode. The AFM is calibrated with a silicon grating with 28nm pitch. The long dimension of an origami tile (parallel to the DNA helices) is used as a subsidiary standard to determine the scale bars shown, which are consistent with the AFM calibration within the expected error. 76 % of 127 tiles with hairpin markers imaged were oriented such that stators faced towards the mica surface.

**Image registration.** Sequential AFM images showed drift of the origami tiles within the imaging scan area. To correct movies with a large amount of drift, origami images

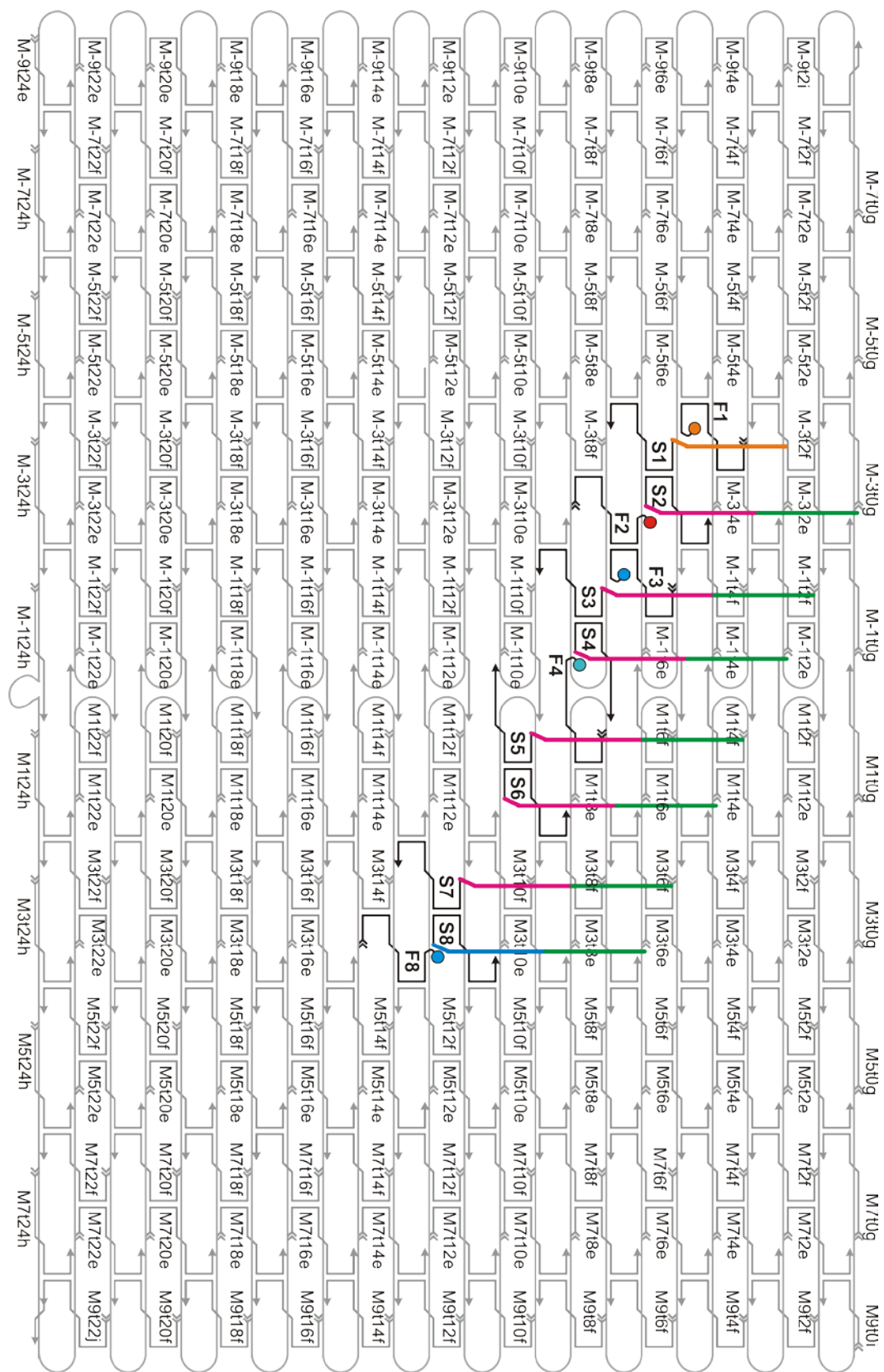
were registered using MatLab Image Processing Toolbox. In this process, 4-6 control points, corresponding to hairpins on the DNA tile, were selected and their locations used to transform the target frame by linear translation, rotation and scaling to match a reference frame. Control points were selected by eye, and their location improved by maximizing the cross-correlation of a small area around the selected point in both images. To correct movies with only a small amount of drift, images were registered with a linear translation using the Turboreg function in ImageJ<sup>3</sup> software.

**Kymograph analysis.** In order to analyze the stepping behavior of the DNA motors, kymographs were created using the Kymograph plugin of ImageJ Image analysis software<sup>3</sup>. AFM height measurements, averaged over a width of 5 pixels along a line corresponding to the DNA motor track, were stacked to create a 2D image. In the resulting kymograph, stationary features, such as hairpins or tile edges, appear as vertical lines and moving features, such as the DNA motor, appear as diagonal lines. The location of the motor in each image was approximated by the position of the maximum measured height along the motor track. Control kymographs were plotted along the rows of hairpins on the track tiles to confirm the correct registration of image frames (Supplementary Fig. 14).

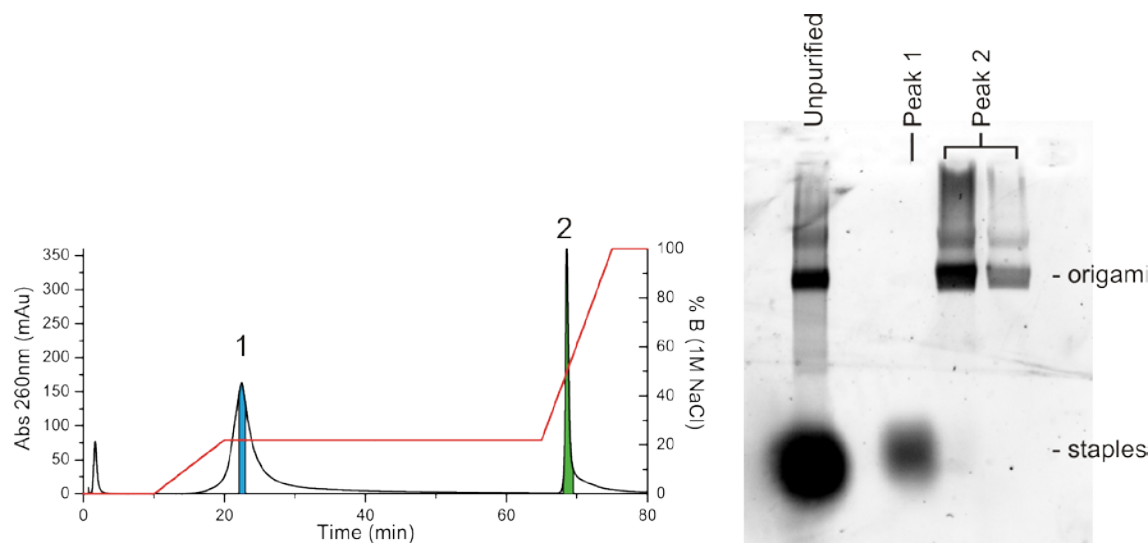
## 2. Supplementary Figures 1 to 14.



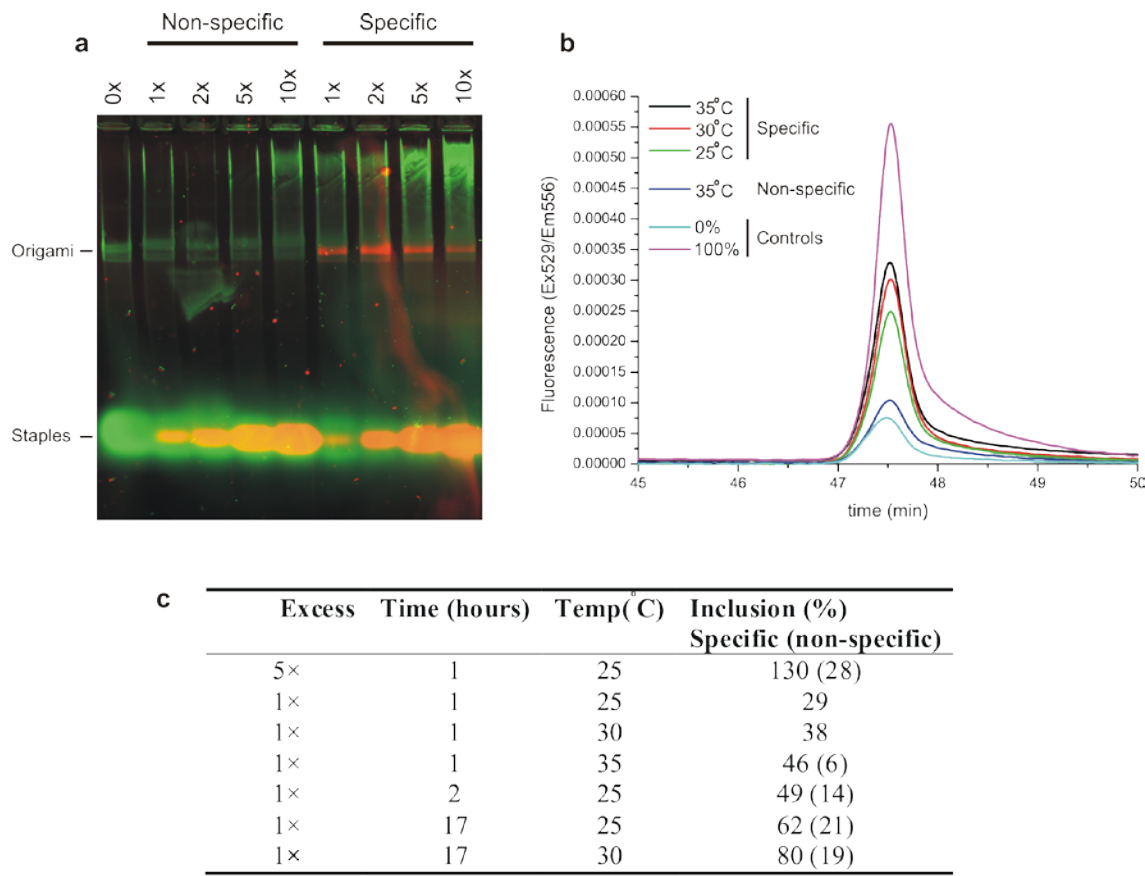
**Supplementary Figure 1.** Origami track design for AFM measurements (tile type A)



**Supplementary Figure 2.** Origami track design for fluorescence measurements (tile type B).



**Supplementary Figure 3.** Ion-exchange HPLC of DNA origami. The DNA absorption signal (left) shows clear separation between staples (1) and DNA origami tiles (2) in a NaCl gradient (red). Analysis by agarose gel electrophoresis (right) confirms that peaks 1 and 2 correspond to staples and origami tiles respectively. Two sequential fractions from peak 2 were loaded in lanes 3 and 4.



**Supplementary Figure 4.** Origami tile repair. The ability of DNA origami tiles to repair themselves without high-temperature annealing was investigated by incubating a tile, assembled with a single missing staple, with the missing staple at a range of concentrations. The staple was labeled with a fluorophore (JOE). **a**, Agarose gel electrophoresis of DNA origami tiles, lacking one staple, incubated with a fluorophore-labeled staple at 37 °C. The fluorescent staple migrates with the origami band if it matches the sequence of the missing staple ('Specific' lanes) and not otherwise ('Non-specific'). **b**, Quantification of staple incorporation by HPLC. The fraction of defective tiles that are repaired by incorporation of the fluorescently labeled staple is estimated by comparing the fluorescence intensity, integrated over the origami peak and normalized by a measurement of DNA absorption (at 260 nm), to the corresponding signal for a tile prepared with the staple present during initial assembly (5× excess) (100% control). Non-specific interaction is also quantified, and is minimal for these conditions. **c**, Repair efficiencies were measured for a range of conditions, and used to optimize the conditions used for loading the S<sub>1</sub>+motor duplex.

**a** Motors stepping forward:

$$\begin{aligned}\frac{dc_1(t)}{dt} &= -k_1 c_1(t) \\ \frac{dc_{i+1}(t)}{dt} &= k_i c_i(t) - k_{i+1} c_{i+1}(t) \\ \frac{dc_8(t)}{dt} &= k_7 c_7(t)\end{aligned}$$

Motors stepping backward:

$$\begin{aligned}\frac{dc_1(t)}{dt} &= k_2 c_2(t) \\ \frac{dc_i(t)}{dt} &= k_{i+1} c_{i+1}(t) - k_i c_i(t) \\ \frac{dc_8(t)}{dt} &= -k_8 c_8(t)\end{aligned}$$

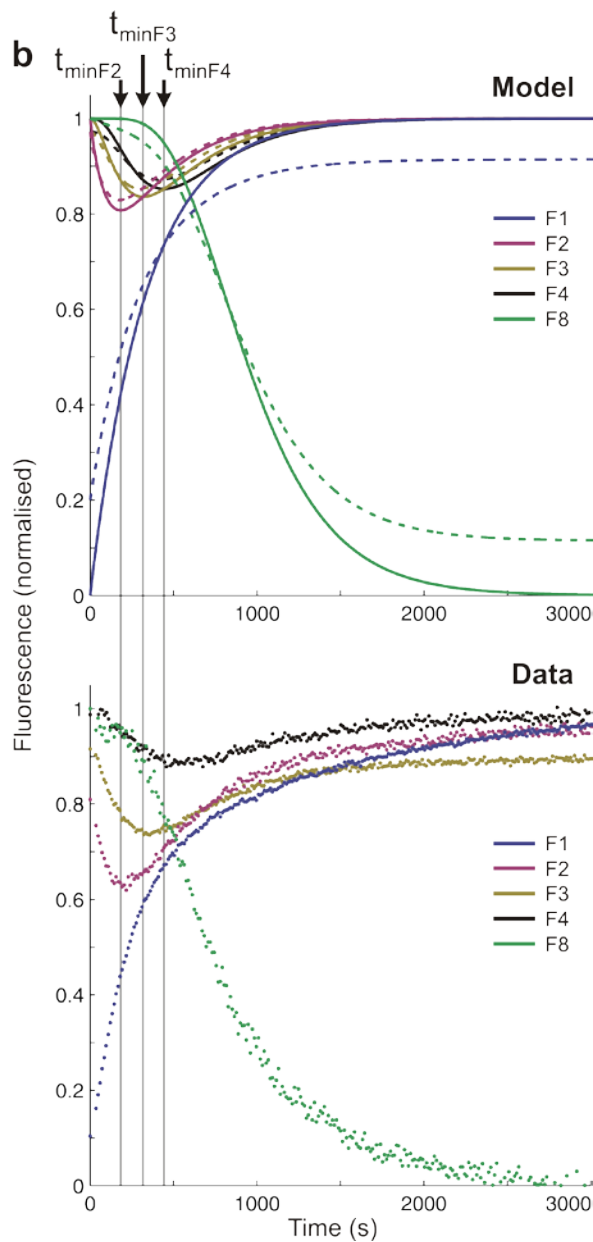
$$k_1 = 0.003 s^{-1}$$

$$k_{2-7} = 0.009 s^{-1}$$

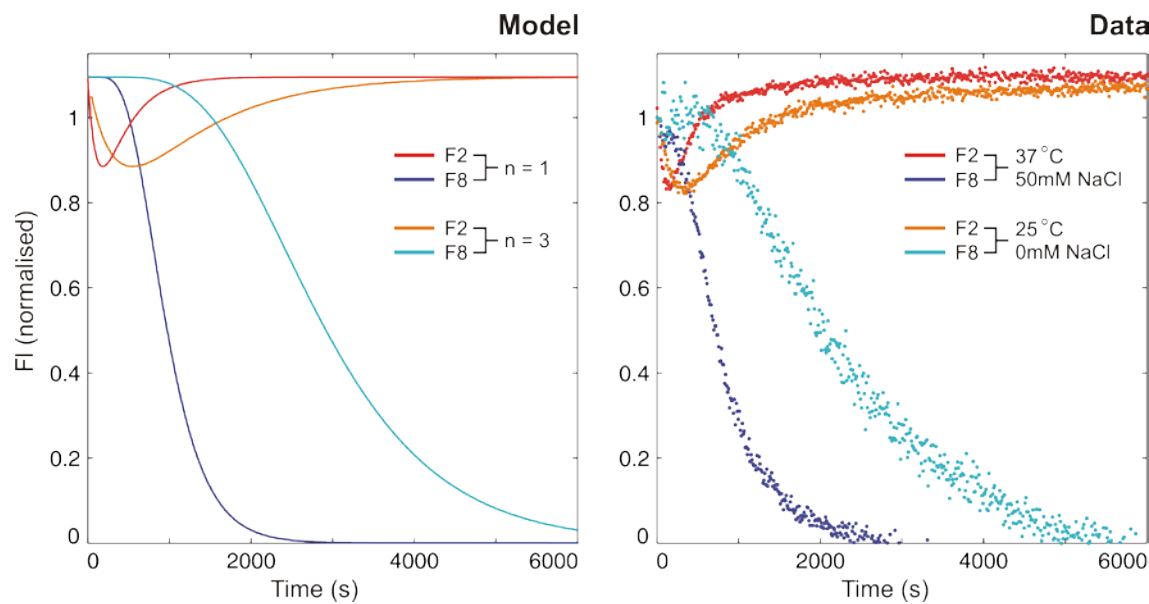
$$k_8 = 0$$

**c**

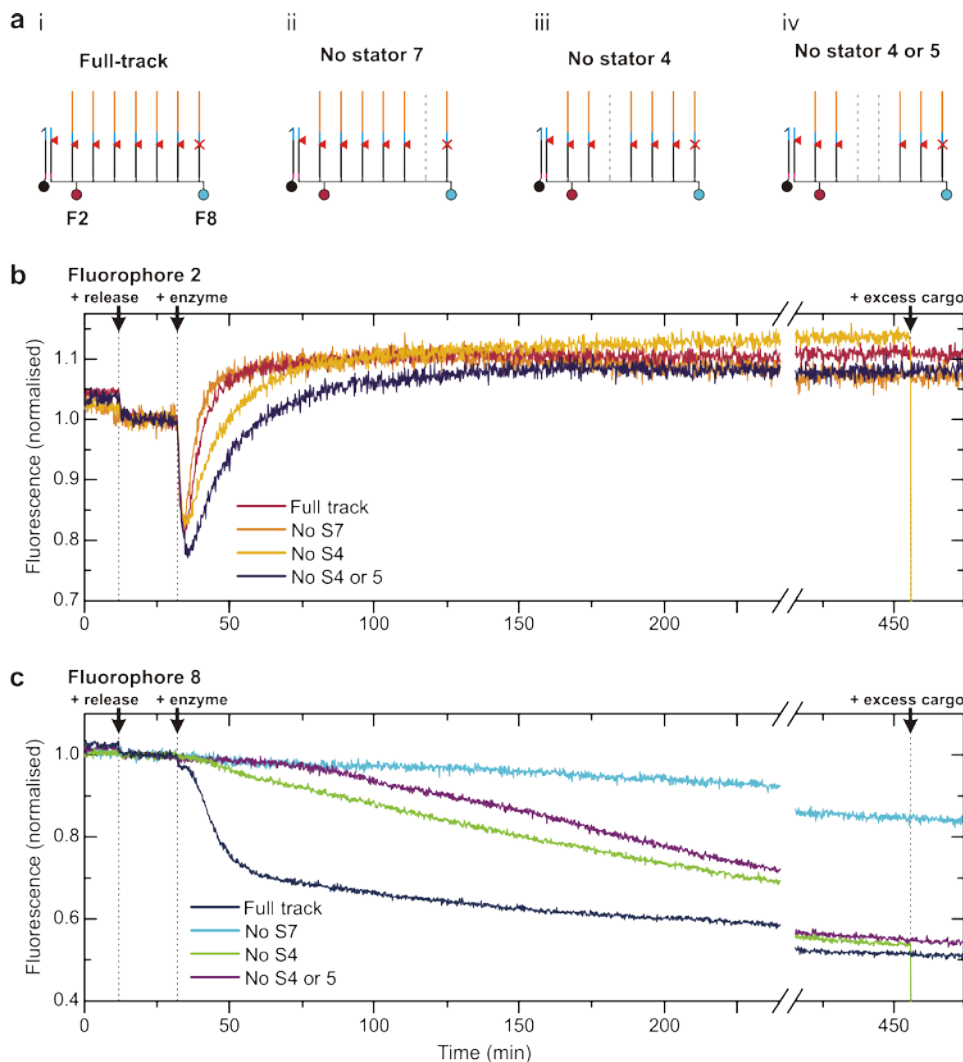
	Model (s)	Data (s)
$t_{\frac{1}{2}F_1}$ (F <sub>1</sub> increase to 50%)	231	$230 \pm 10$
$t_{\min F_2}$ (F <sub>2</sub> is min.)	183	$200 \pm 50$
$t_{\min F_3}$ (F <sub>3</sub> is min.)	317	$370 \pm 10$
$t_{\min F_4}$ (F <sub>4</sub> is min.)	443	460
$t_{\frac{1}{2}F_8}$ (F <sub>8</sub> fall to 50%)	929	$700 \pm 50$



**Supplementary Figure 5.** Kinetic model for stepping rate analysis. **a**, Unidirectional movement of the motor along the track is modeled using first-order rate constants taken from measurements at 37 °C on a short track with 3 stators<sup>4</sup>. **b**, Predicted time-dependence of normalized fluorescence signals ( $1-c_i(t)$ ) ( $i=1,2,3,8$ ) and corresponding data, recorded at 37 °C (Fig. 2). Vertical lines indicating the times at which F<sub>2</sub>, F<sub>3</sub> and F<sub>4</sub> are a minimum are a guide to the eye. Solid calculated curves correspond to the ideal case, in which all motor is loaded at S<sub>1</sub>. A second case (broken lines) is considered, in which 20% of motor is distributed evenly over stators S<sub>2</sub>–S<sub>8</sub> before the motor is activated. Motor loaded in the middle of the track is given an equal chance of taking an initial forward or backward step, after which it is restricted to one direction. In this case the latent period before F<sub>8</sub> fluorescence begins to decay is reduced, as observed. **c**, Experimental data are in quantitative agreement with the predictions of the model. Minima for F<sub>2</sub>, F<sub>3</sub> and F<sub>4</sub> occur sequentially.



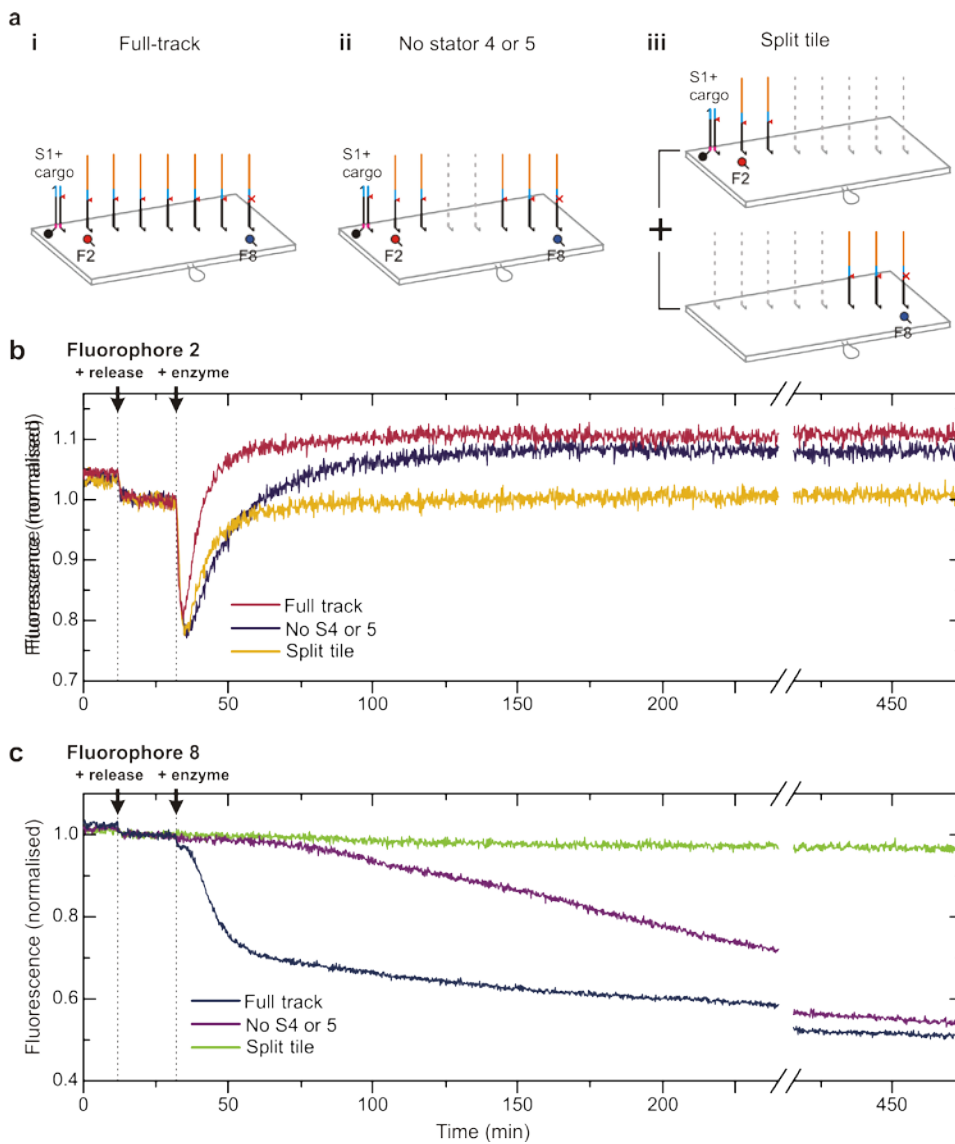
**Supplementary Figure 6.** Dependence of stepping rate on temperature and buffer conditions. Model predictions for  $F_2$  and  $F_8$  fluorescence (Supplementary Figure 5) with rate constants reduced by a factor  $n$ . Data corresponds to two different sets of experimental conditions: 37 °C with buffer used for fluorescence experiments (1x TAE, 12.5mM magnesium acetate, 50mM sodium chloride); 25 °C, omitting the sodium chloride from the buffer. The data are consistent with a 3-fold reduction in stepping rate in the latter case. The AFM data presented in Figures 3 and 4 was recorded at 23 °C in a similar, sodium-free buffer: a 4-fold reduction in published<sup>4</sup> rate constants was used to model the slower transport observed in these AFM experiments.



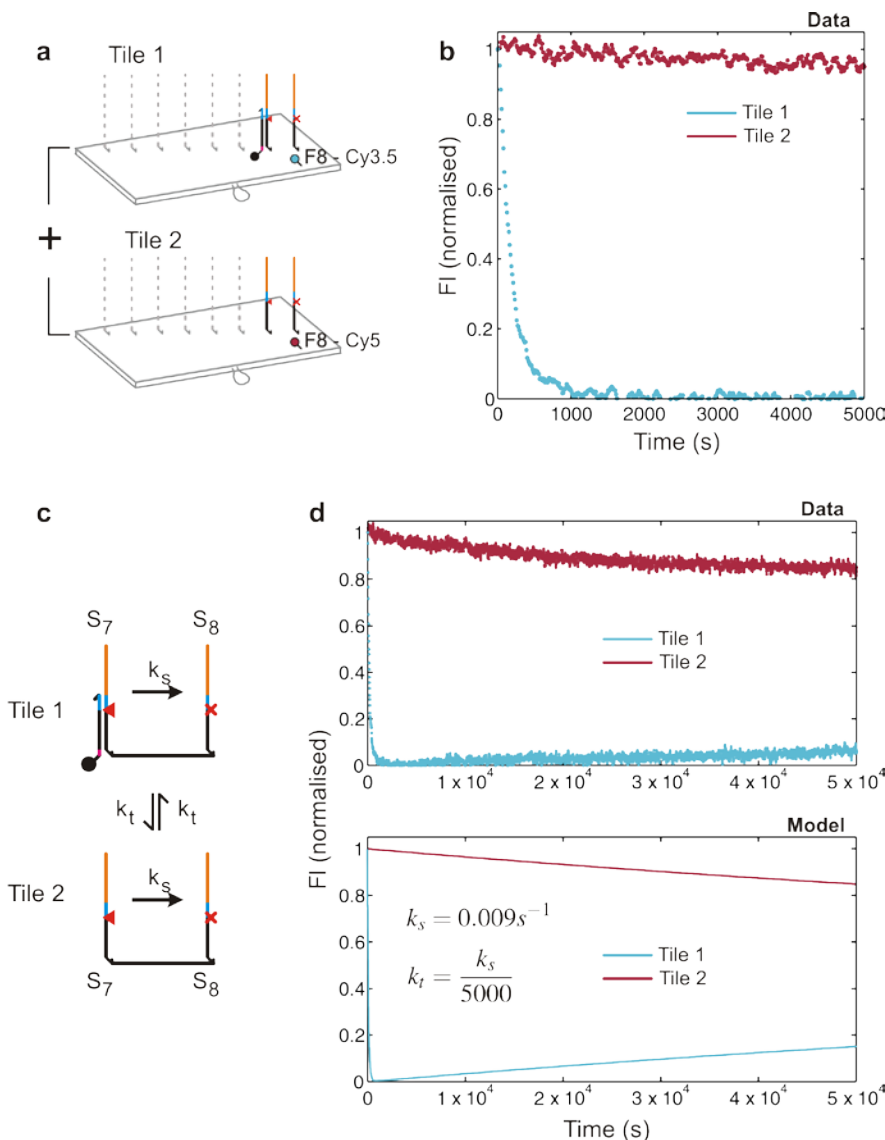
**Supplementary Figure 7.** Stepping along gapped tracks. **a**, Tracks compared: (i) full track ( $S_{1-8}$ ), and tracks broken by omitting (ii) stator  $S_7$ , (iii) stator  $S_4$ , and (iv) stators  $S_4$  and  $S_5$ . Staples bearing the omitted stators were replaced with unmodified staples. **b,c**, Fluorescence from fluorophores  $F_2$  (b) and  $F_8$  (c) on each track was recorded at 37°C.

The rate of quenching of  $F_8$  fluorescence, indicating arrival of the motor at the end of the track, is reduced for damaged tracks, as expected. Nevertheless, some decrease in  $F_8$  fluorescence, indicating delayed arrival of motor molecules at the final stator, was observed for all tracks. The decrease in arrival rate is greater in the case of a track with an 18 nm gap, produced by omitting both  $S_4$  and  $S_5$ , than in the case of a 12 nm gap, produced by omitting  $S_4$  only. We infer that motor strands can cross a gap in a track at a rate that depends on the gap size. Comparison with predictions of the model presented in Supplementary Fig. 5, modified to include a slow step, leads to an estimate of a 50× reduction in stepping rate across a 12 nm gap, and a 100× reduction for an 18 nm gap.

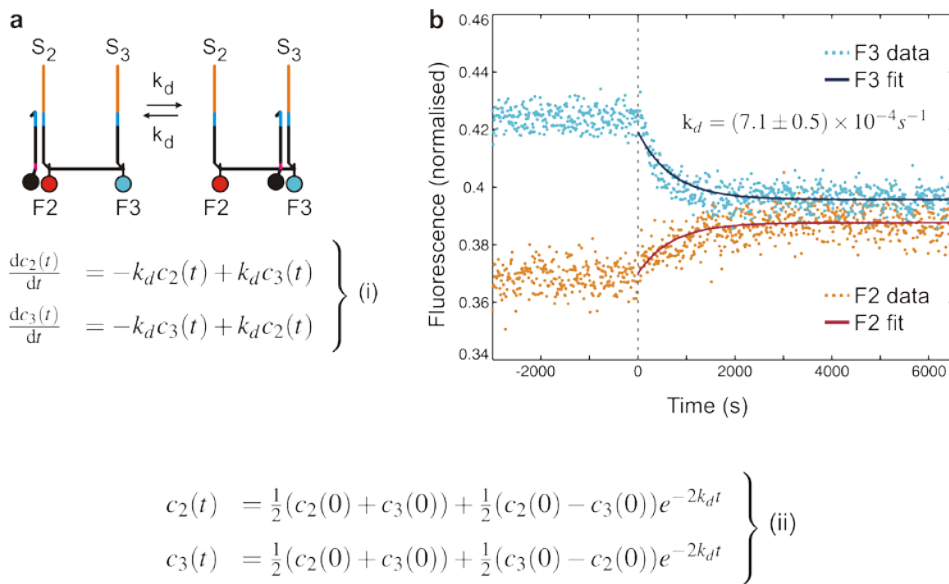
Motors reach  $S_8$  at a faster rate for tracks broken in the middle ( $S_4$ ) than for tracks broken at the end ( $S_7$ ). To step directly from  $S_6$  to  $S_8$  the motor must step onto a mismatched stator with a lower affinity for the motor, resulting in a further reduction in rate of transfer across the gap.



**Supplementary Figure 8.** The extent of inter-molecular transfer of motor for a ‘split-tile’ sample. **a**, Three tracks are compared: (i) complete, (ii) broken by omitting stators  $S_4$  and  $S_5$ , and (iii) a matching split-tile sample containing a mixture of two types of tile carrying incomplete tracks. Tracks (i) and (ii) were labeled at stators  $S_2$  and  $S_8$ . In the split-tile sample, the first tile type carries stators  $S_1$  to  $S_3$ , with fluorophore  $F_2$ , and is loaded with the motor on stator  $S_1$ . The second type carries stators  $S_6$  to  $S_8$ , and  $F_8$ , and has no motor. The two tile types are combined, and observed together. Measurements were made at 37 °C. **b**, Fluorescence from fluorophore  $F_2$  shows transient quenching as the motor moves past this position in all samples, as expected, showing that the motor mechanism is not disrupted in the split-tile sample. **c**, Fluorescence from fluorophore  $F_8$  at  $S_8$ . Quenching of the  $F_8$  signal in the split-tile sample is much less than that observed for the track broken at stators  $S_4$  and  $S_5$ . We conclude that inter-tile transfer is slow, and almost all of the motor that reaches stator  $S_8$  in damaged tracks is crossing the gap in an intramolecular step.

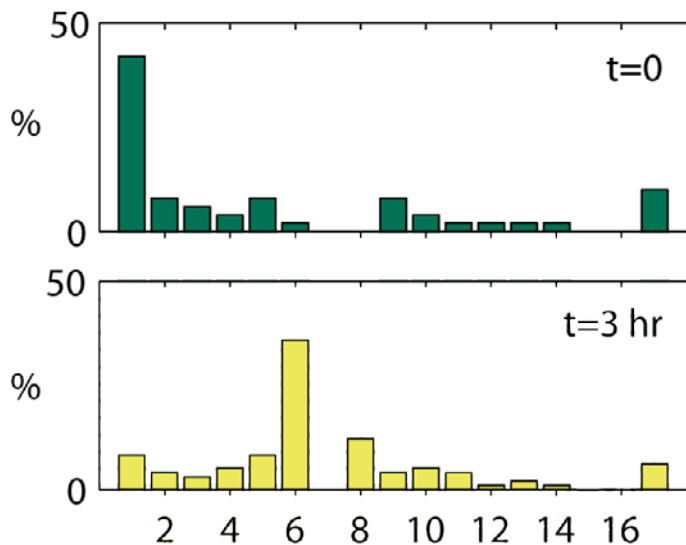


**Supplementary Figure 9.** Rate of motor transfer between tiles. **a** Two-stator tracks ( $S_7$ ,  $S_8$ ) were used to quantify intermolecular transfer. Tile 1 was labelled with Cy3.5 and Tile 2 with Cy5, both at  $S_8$ . Motor was loaded at  $S_7$  on Tile 1 by insertion of the motor- $S_7$  duplex.  $S_8$  was blocked during loading, mixed with an equal amount of Tile 2 (final concentration  $\sim 12.5\text{nM}$  for each tile type) and unblocked by incubation with the release strand before addition of enzyme ( $t = 0$ ). **b**, Initial rates of change of fluorescence from the  $S_8$  labels indicate that stepping between stators on the same track is much quicker than transfer between tiles. **c**, As a first approximation the system can be modeled by two rates, for intra-tile stepping and inter-tile transfer ( $k_s$  much larger than  $k_t$ ). **d**, The data is consistent with a transfer rate of order  $5000\times$  smaller than the stepping rate. On the time scale of motor movement, transfer of motor between tracks is negligible.

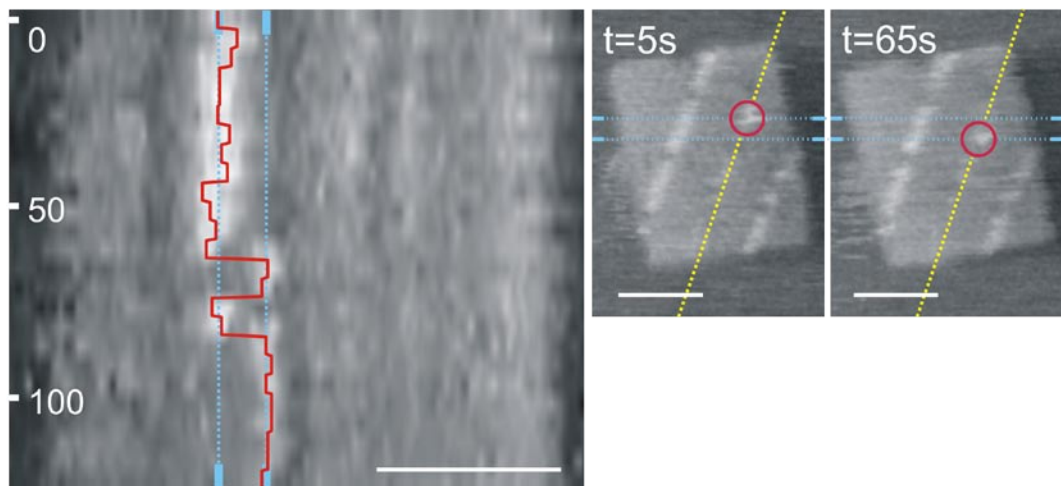


**Supplementary Figure 10.** Rate of motor diffusion along the track. **a** Simplified tracks with only two identical stators,  $S_2$  and  $S_3$ , were used to quantify the rate of motor diffusion between stators. Equal amounts of tracks labeled with either  $F_2$  or  $F_3$  were combined and observed in the same measurement. **b**, Motor was loaded preferentially on  $S_2$  by insertion of the  $S_2$ -motor duplex while blocking stator  $S_3$ . The corresponding unblocking strand was added ( $t = 0$ ) and diffusion of the motor observed. The reversible diffusion reaction is modeled by a simple set of differential equations (i) with an analytical solution (ii). A fit to both sets of data,  $F_2$  and  $F_3$  fluorescence, yields an estimate for the rate constant for undriven stepping  $k_d$  that is  $13\times$  slower than the stepping rate  $k_s$ .

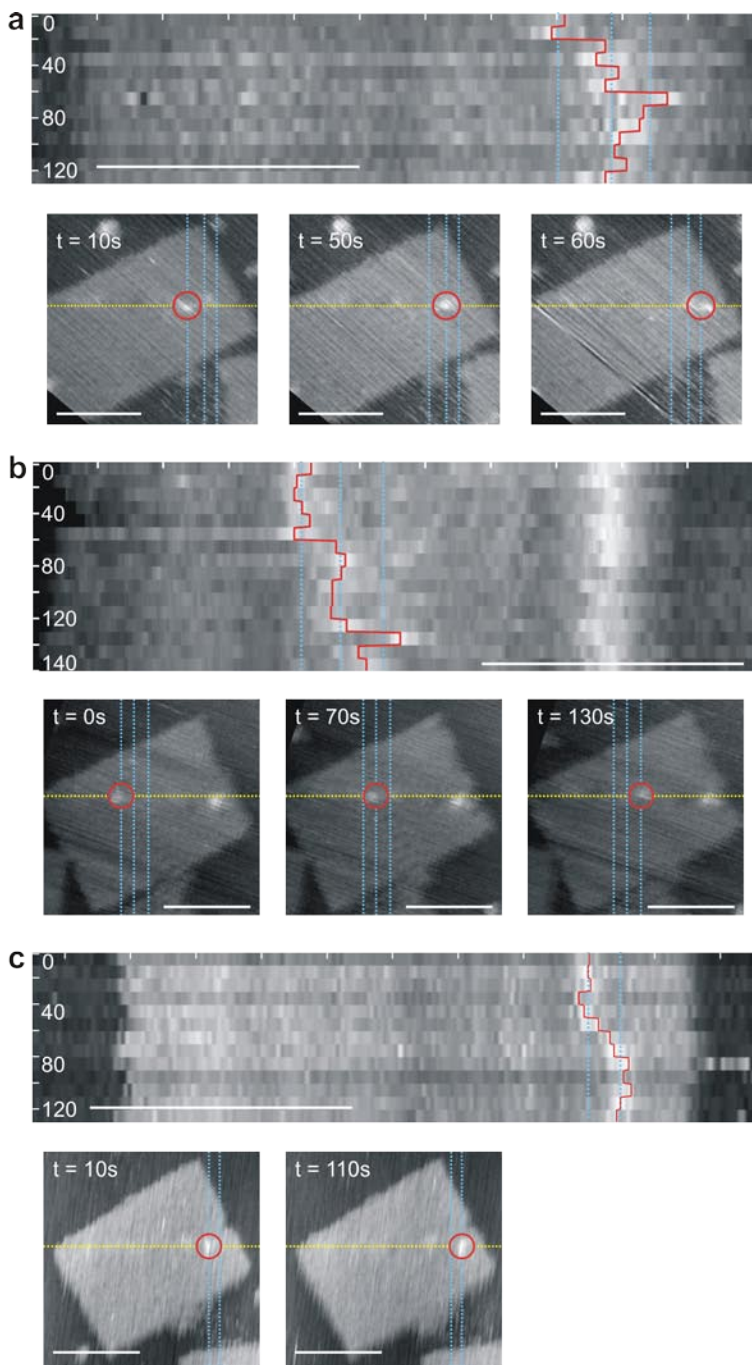
In all other measurements the motor is loaded on a stator that has an additional 2-nt overlap with the motor. This additional overlap helps to maintain a strong bias of the motor population to the initial stator until the stator is cut on addition of enzyme. In this case the two stators are identical and only a small bias in motor loading was possible.



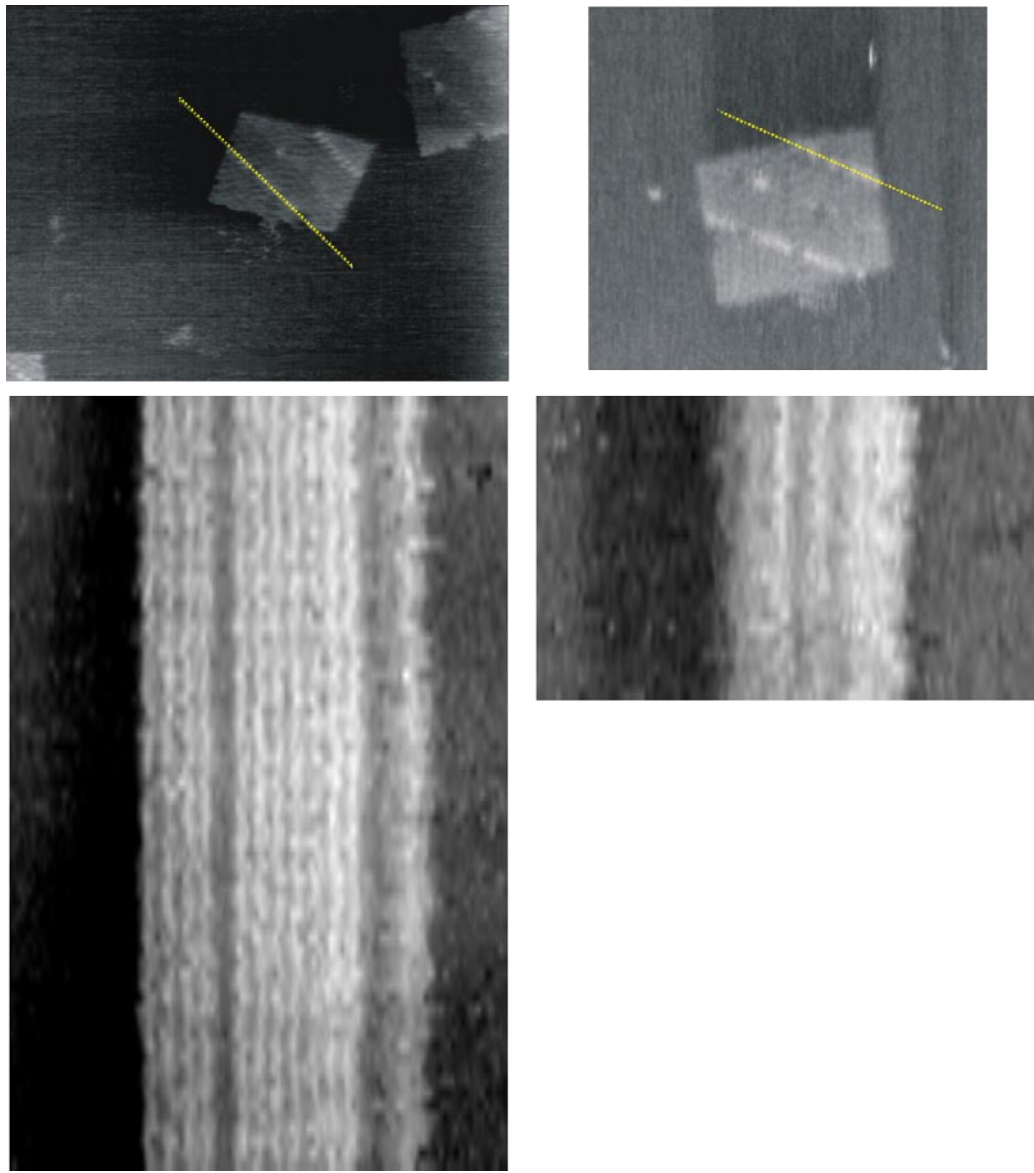
**Supplementary Figure 11.** The motor pauses before a missing stator on broken tracks. Broken tracks were prepared by assembling tiles without stator S<sub>7</sub>, which was replaced by an unmodified staple, leaving a 12 nm gap between S<sub>6</sub> and S<sub>8</sub>. Motor was loaded at S<sub>1</sub> and the tiles were incubated with nicking enzyme at 23°C for 3 hours. The position of the motor on the track before and after addition of enzyme was determined by AFM (51 tiles were counted at  $t=0$  and 98 at  $t=3\text{ hr}$ ). The observed distributions of motor positions show that the motor moves from S<sub>1</sub> (41% at  $t=0$ ) to S<sub>6</sub> (36% at  $t=3\text{ hr}$ ) but is largely unable to cross the gap left by the missing S<sub>7</sub> on this time scale. The experiment demonstrates that motor moves sequentially between adjacent stators and that the motor population initially builds up at the last stator before a gap in the track.



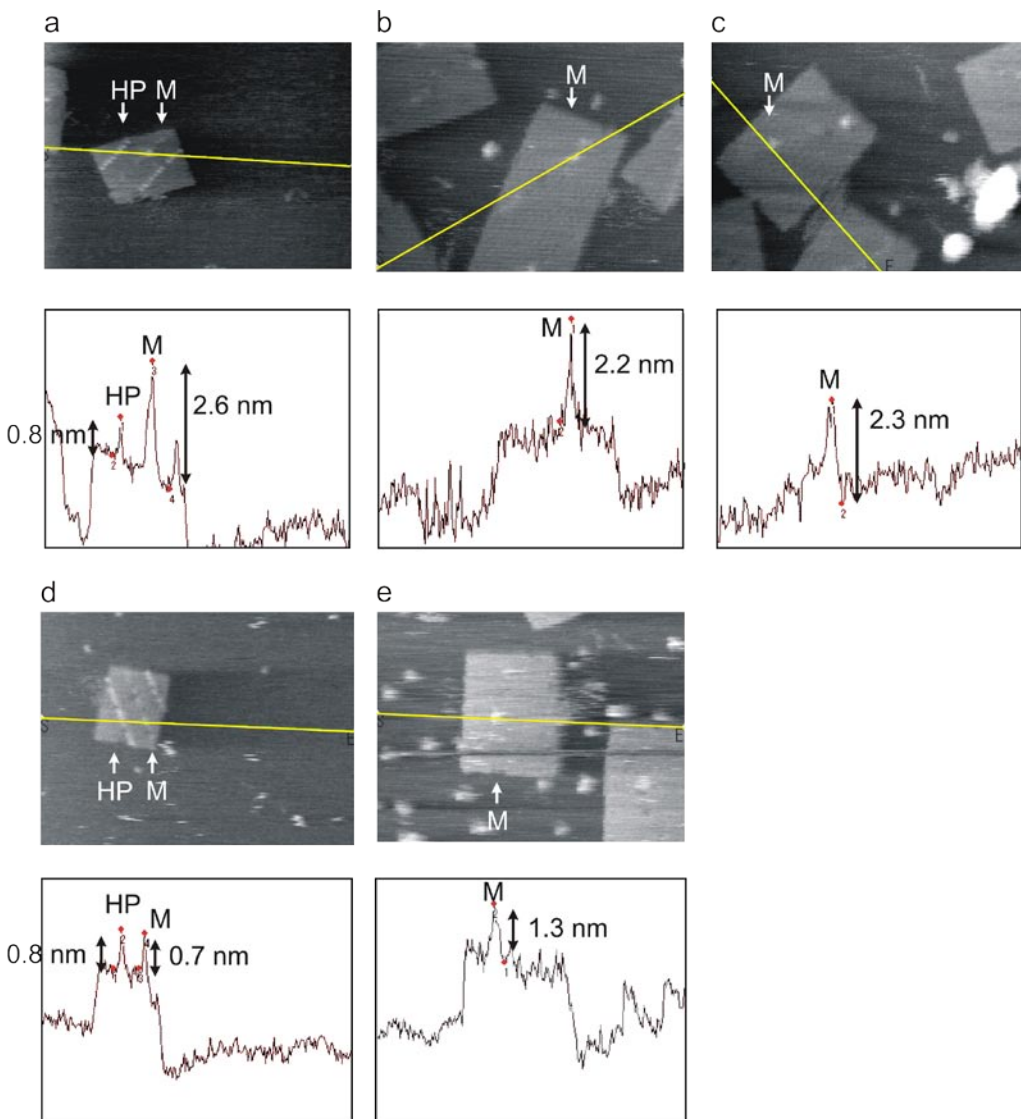
**Supplementary Figure 12.** Kymograph showing discrete steps of a single motor molecule between two adjacent stators (Supplementary Movie 2). Images were processed as for Figure 4. Scale bars are 50 nm, time scale for the kymograph is in seconds.



**Supplementary Figure 13.** Kymographs and image frames showing discrete steps of a single motor molecule from three additional AFM movies in which stepping between three (**a,b**) and two (**c**) adjacent stators is observed. These tiles are of type A, without hairpin markers. Images were processed as for Figure 4. Scale bars are 50 nm, time scales are in seconds.



**Supplementary Figure 14.** Kymograph controls. Kymographs, showing the evolution of rows of hairpin topological labels, were constructed from AFM movies. Single frames (top) show selected loci (straight yellow lines), running along lines of hairpin-modified staples, for which the two kymographs (bottom) were constructed. The hairpins, which are stationary, appear as vertical lines in the kymograph, confirming that the image registration process used to align the frames of the image sequences operates correctly.



**Supplementary Figure 15.** Height profiles from AFM movies. **a, b, c,** Movies with at least one completed step, corresponding to kymographs in Figure 4 and Supplementary Fig. 13a and 13b respectively. **d,e** Movies with no completed steps, corresponding to kymographs in Supplementary Figs 12 and 13c. Single frames (top) show a line (yellow), passing through the motor position, along which the height profile (bottom) is plotted. Measured heights of hairpins (HP) and motors (M) are indicated. In movies showing completed steps, but not in the single-step movies, the height of the motor is significantly greater than that of a hair-pin. This observation is consistent with our interpretation that completed steps between stators are a result of the action of enzyme that remains bound to the motor, whereas reversible transitions between adjacent stators do not require the presence of enzyme.

### 3: Supplementary Tables

Staple strands modified for AFM experiments (Supplementary Figure 1). For use with tile type A <sup>1</sup> .	
S1	<b>GGAACCTCAGCCCCACTAACATCGTTGAGAATAGCTTTCGGGATCGTCGGTAGCA</b>
S2	<b>GGAACCTCAGCCCCACTAACATTTAAAGGCCGAAAGGAACAACAAAGCTTCCAG</b>
S3	<b>GGAACCTCAGCCCCACTAACATTTTTTCACTGAAAATTGTGTCGAAATCTGTACAGA</b>
S4	<b>GGAACCTCAGCCCCACTAACATTTCCGCTGATGGAAGTTCCATTAAACATAACCG</b>
S5	<b>GGAACCTCAGCCCCACTAACATTTAGTAATCTAAATTGGGCTTGAGAGAATACCA</b>
S6	<b>GGAACCTCAGCCCCACTAACATTTACGAGTAGTGACAAGAACCGGATATACCAAGC</b>
S7	<b>GGAACCTCAGCCCCACTAACATTTGGAATTACTCGTTACAGACGACAAAAGATT</b>
S8	<b>GGAACCTCAGCCCCACTAACATTTCTAACCCGAGGCATAGTAAGAGCTTTTAAG</b>
S9	<b>GGAACCTCAGCCCCACTAACATTTCTAATTACGCTAACGAGCGTCTATATCGCG</b>
S10	<b>GGAACCTCAGCCCCACTAACATTTCTTACCCAGCCAGTTACAAAATAATGAAATA</b>
S11	<b>GGAACCTCAGCCCCACTAACATTTGGTATTAAGAACAAAGAAAATAATTAAAGCCA</b>
S12	<b>GGAACCTCAGCCCCACTAACATTTTAAGCCTACCAAGTACCGCACTTTAGTTGC</b>
S13	<b>GGAACCTCAGCCCCACTAACATTTCATATTAGAAATACCGACCCTGTTACCTTT</b>
S14	<b>GGAACCTCAGCCCCACTAACATTTAATGGTTACAACGCCAACATGTAGTTCAGCT</b>
S15	<b>GGAACCTCAGCCCCACTAACATTTTATGTAACACCTTTTAATGGAAAATTACCT</b>
S16	<b>GGAACCTCAGCCCCACTAACATTTTGAATTATGCTGATGCAAATCCACAAATATA</b>
S17	<b>GGA<u>ACT</u>T<u>CAG</u>CCCCACTAACATTTAAACAAATTCAATATAATCCTATCAGAT</b>
Hp1	<b>TGCCTTGACTGCCTAT<u>TCCT</u>TTTGAGGAACAAGTTTCTTGT<u>TCGG</u>AACAGGGATAG</b>
Hp2	<b>CTGAAACAGGTAA<u>TA</u><u>TC</u>CTTTGAGGAACAAGTTTCTTGT<u>GT</u>TTAACCCCTCAGA</b>
Hp3	<b>GTTTGCCACCTCAGAG<u>TC</u>CTTTGAGGAACAAGTTTCTTGT<u>CC</u>CCACCGATA<u>AG</u>GG</b>
Hp4	<b>CACCA<u>AG</u>GT<u>TC</u>GGT<u>CA</u><u>TC</u>CTTTGAGGAACAAGTTTCTTGT<u>TT</u>AG<u>CCC</u>CC<u>GG</u>CAGCAA</b>
Hp5	<b>TCACAA<u>CT</u>CG<u>AC</u><u>TC</u>CTTTGAGGAACAAGTTTCTTGT<u>GT</u>ATTACCATCGTTCA</b>
Hp6	<b>CCGGAA<u>AC</u>AC<u>CC</u>AC<u>CG</u><u>TC</u>CTTTGAGGAACAAGTTTCTTGT<u>GA</u>ATA<u>AG</u>TA<u>AG</u>ACTCC</b>
Hp7	<b>TGAACAA<u>AC</u>AG<u>T</u><u>AT</u><u>GT</u><u>TC</u>CTTTGAGGAACAAGTTTCTTGT<u>TT</u>AGCAA<u>ACT</u>AAA<u>AG</u>AA</b>
Hp8	<b>TACATACATTGACGGGAG<u>TC</u>CTTTGAGGAACAAGTTTCTTGT<u>TA</u>TTAA<u>ACT</u>ACAGGGAA</b>
Hp9	<b>ATATA<u>AT</u>TTT<u>TC</u>ATT<u>GA</u><u>AT</u><u>TC</u>CTTTGAGGAACAAGTTTCTTGT<u>TC</u>CC<u>CC</u>CT<u>CA</u>AT<u>CG</u>T<u>CA</u></b>
Hp10	<b>AAACAGTTGATGGCTT<u>TC</u>CTTTGAGGAACAAGTTTCTTGT<u>AG</u>GT<u>CT</u>T<u>TT</u>AA<u>AT</u>A</b>
Hp11	<b>CAAA<u>AT</u>TA<u>AG</u>T<u>AC</u>GG<u>TC</u>CTTTGAGGAACAAGTTTCTTGT<u>GT</u>T<u>GT</u>CT<u>GG</u>A<u>AG</u>GT<u>TC</u>A</b>
Hp12	<b>TCC<u>AT</u>AC<u>AT</u>AC<u>AG</u><u>GT</u><u>TC</u>CTTTGAGGAACAAGTTTCTTGT<u>CA</u>AG<u>GC</u>AA<u>CT</u>TT<u>AT</u>TT</b>
Hp13	<b>GGTAG<u>CT</u>GG<u>AT</u>AAA<u>TC</u>CTTTGAGGAACAAGTTTCTTGT<u>AT</u>TT<u>TA</u>AC<u>AT</u>C</b>
Hp14	<b>TAT<u>AT</u>TT<u>TA</u>GT<u>GA</u><u>AT</u><u>TC</u>CTTTGAGGAACAAGTTTCTTGT<u>TA</u>TT<u>AT</u>GT<u>GT</u>T<u>AA</u></b>
Hp15	<b>AA<u>AT</u>AA<u>TT</u>AA<u>AT</u>TG<u>TC</u>CTTTGAGGAACAAGTTTCTTGT<u>AA</u>AC<u>GT</u><u>GT</u><u>AT</u>TT<u>CA</u></b>
Hp16	<b>GTT<u>AA</u><u>AA</u><u>TT</u>AA<u>CC</u>A<u>TC</u>CTTTGAGGAACAAGTTTCTTGT<u>AT</u>AG<u>GA</u>AC<u>CC</u><u>GG</u><u>AC</u>C</b>
Hp17	<b>TT<u>CG</u><u>CC</u><u>AT</u><u>TG</u><u>CC</u><u>GG</u><u>AA</u><u>TC</u>CTTTGAGGAACAAGTTTCTTGT<u>AC</u>AG<u>GG</u><u>CA</u>AC<u>AG</u><u>T</u><u>AC</u></b>
Hp18	<b>CTTT<u>AC</u><u>AC</u><u>AG</u><u>AT</u><u>GA</u><u>AA</u><u>TC</u>CTTTGAGGAACAAGTTTCTTGT<u>TA</u>AC<u>AG</u><u>TA</u>AG<u>CG</u><u>CC</u>A</b>
Hp19	<b>GG<u>AT</u>TT<u>AG</u><u>CG</u><u>GT</u><u>AT</u>AA<u>TC</u>CTTTGAGGAACAAGTTTCTTGT<u>AT</u>CC<u>TT</u>GT<u>TT</u>CA<u>GG</u></b>
Hp20	<b>TT<u>AT</u>TA<u>AT</u><u>GC</u><u>GT</u><u>CA</u><u>AT</u><u>TC</u>CTTTGAGGAACAAGTTTCTTGT<u>TT</u>AG<u>AT</u>TA<u>CT</u>AG<u>AG</u><u>GT</u></b>
Hp21	<b>GA<u>AT</u>GG<u>CT</u><u>AG</u><u>GT</u><u>AT</u>AA<u>TC</u>CTTTGAGGAACAAGTTTCTTGT<u>AC</u>CG<u>GC</u><u>CT</u><u>CA</u>AC<u>TA</u>AT</b>
Hp22	<b>GCC<u>AC</u><u>GC</u><u>CT</u><u>AT</u><u>AC</u><u>GT</u><u>GG</u><u>TC</u>CTTTGAGGAACAAGTTTCTTGT<u>CA</u>AG<u>AC</u><u>AC</u><u>GT</u><u>CT</u><u>CAT</u></b>
Hp23	<b>GG<u>AA</u><u>AT</u><u>AC</u><u>CT</u><u>AC</u><u>AT</u><u>TT</u><u>TC</u>CTTTGAGGAACAAGTTTCTTGT<u>TG</u><u>AC</u><u>GT</u><u>CT</u><u>AC</u><u>CT</u><u>GA</u><u>AA</u></b>
motor	<b>CG<u>AT</u>GT<u>TT</u><u>AG</u><u>TT</u><u>GG</u><u>GT</u><u>GA</u><u>GG</u><u>TT</u><u>CC</u></b>

Staple strands modified for fluorescence experiments (Supplementary Fig. 2). For use with tile type B (Supplementary Table 2).

S1	<b>GGAACCTCAGCCCAACTAACATCG</b> TTTGCTCATTCTTATGCGATTAAAGCGAGGCAT
S2	TCTTGTACCGTTGCAGACT <b>GGAACCTCAGCCCAACTAACAT</b> TTTGAATTACCAGTGAATAAGGCTTGTGCAAATC
S3	TCTTGTACCGTTGCAGACT <b>GGAACCTCAGCCCAACTAACAT</b> TTTACAGACGGCAAAAGAAGTTTGTGTTAATT
S4	TCTTGTACCGTTGCAGACT <b>GGAACCTCAGCCCAACTAACAT</b> TTTAGGCTTTACGATAAAAACCAAAATTAAAGAC
S5	TCTTGTACCGTTGCAGACT <b>GGAACCTCAGCCCAACTAACAT</b> TTTACAGAGGTCAAAATGAAAATAGGAAGCAA
S6	TCTTGTACCGTTGCAGACT <b>GGAACCTCAGCCCAACTAACAT</b> TTTGTTAACGAATAACATAAAAACATAAACG
S7	TCTTGTACCGTTGCAGACT <b>GGAACCTCAGCCCAACTAACAT</b> TTGGCTTATCGCACTCATCGAGAACCCGACAAA
S8	TCTTGTACCGTTGCAGACT <b>GGAACCCAGCCCAACTAACAT</b> TTCAAGTACCGGTATTCTAAGAACGCCATATTA
block	<b>GGTTCC</b> AGTCTGCAAACGGTACAAGA <b>AAGTCGCTTCGCACA</b>
release	<b>TGTGCGAAGCGACTT</b> TCTTGTACCGTTGCAGACT <b>GGAACC</b>
motor	IowaBlackRQ-CGATGTTAGTGGCTGAGGTTCC
F1	AAACACTGCTCCATGTTACTAACAAAGCT-JOE
F2	GGTAATAGCAACACTATCATAACATCATTGT-Cy5
F3	AGAAACACTTTAATTCAACTTACCTCGTT-Cy3.5
F4	TCCTTATTAAAAGAACTGGCATGATAGCGAG-Cy3.5
F8	TTAATTGATAATTCTGTCCAGACTATTAAAC-Cy3.5

**Supplementary Table 1.** Modified staple strands for AFM and fluorescence experiments. For Tile type A, sequences of unmodified staples are as listed by Rothemund<sup>1</sup>. For Tile type B, sequences of unmodified staples are as listed in Supplementary Table 2. The stator sequence differs slightly from that used previously<sup>4</sup>: the length is 22 nt rather than 24 nt and the nick site is 6 nt from the 5' end rather than 8 nt.

## Unmodified staple strands for reduced twist rectangular origami tile (tile type B)

M1t0g	ATTCCACAGACAGCCCTCATAGTTAGCGTAA	M5t0g	AATAGGAACCCATGTACCGTAACGGGTTGAT
M1t2f	GGATTAGGAGAGGCTGAGACTCCTGCATAACC	M5t2f	ATAAGTATTATAAACAGTTAATGATAAATCC
M1t2e	AAGTATTAAATTAGCGGGGTTTGCCTGTAGC	M5t2e	AGTGCCGAGCCCGGAATAGGTGTGCAAGGCC
M1t4f	GCATTGACGAACCACCACAGAGCGGAGATT	M5t4f	TCATTAACCTCAGAGCCGCCACGTAGCGAC
M1t4e	CGCCACCAAGGAGGTTGAGGCAGAAACATGA	M5t4e	ACCGCCTGCCAGAATGAAAGCTGAGTAAC
M1t6f	TTAGCAAGAACATCACCAGTAGCACATTGGCT	M5t6f	AGAACATCAATATTCACTAAAGGTGACATATAA
M1t6e	GCCAGCAAGCCGAAACGTCACCCCTCAGAGC	M5t6e	ACGGAAATGTTGCCTTACCGTCCACCGGA
M1t8f	TCCTTATTAAAAGAACTGGCATGATAGCGAG	M5t8f	AAGAACCGGCAGATAGCCAAACAAACACCCCT
M1t8e	GAATACCCACGCAGTATGTTAGCGAATTAGA	M5t8e	AAAAGTAACAAAGACACCACGGAAAAATATTG
M1t10f	TACAGAGAGTCAAAATGAAAATAGGAAGCAA	M5t10f	GAACAAAGTTACAAAATAAACAGCGAGGCCT
M1t10e	TGTTAACGAATAACATAAAAACATAAACG	M5t10e	TTTGCCAGTCAGAGGGTAATTGAGTTTTAAG
M1t12f	GCGCCAATTTCATCGTAGGAAAGGTGGCA	M5t12f	TTTAGCGACATTCCAAGAACGGGACGACAA
M1t12e	CGTTTTATAGCAAGCAAATCAGCGATTTT	M5t12e	TTCCCTTACCTCCCGACTTGCAGGAGCCTAA
M1t14f	CCAGTAATATTAGGCAGAGGCAAATATGAT	M5t14f	TAAACAAACAAGCCAACGCTCAACTCATCTTC
M1t14e	AACATGTAAGAGAAATATAAGTAAAGCAAGC	M5t14e	ACCACTATATGTTAGCTAATGCAGGCTGTCT
M1t16f	CCAATCGCTATATGTAATGCTGCCAATAGG	M5t16f	TGACCTAAATCAAAATCATAGGTTGGAAACA
M1t16e	TATATAACAAAGACAAAGAACGCGACAACGCC	M5t16e	GTGAATTATTTAATGGTTGAAAAATTCTT
M1t18f	TCAAGAAAAAGAAGATGATGATTAGGCT	M5t18f	GTACATAATTGCTTGAATACCAAAAGGGTTA
M1t18e	ACCTGAGCACAAAATTAAATTACATGGTTGGT	M5t18e	TCGCCTGAATCAATATATGTGAGAGTCATAA
M1t20f	ATGGCAATATCATATTCTGATTCTAAAGT	M5t20f	GAACCTACAAAAGTTGAGTAACATCTAAAA
M1t20e	GAATTATCTCATCAATATAATCCTTCAATT	M5t20e	TTAATTTCATATCAAATTATTAACGGAT
M1t22f	CAATCAATCTGAACCTCAAATATTGGTCCG	M5t22f	TATCTTAAACCGCCTGCAACAGTGTAGAATA
M1t22e	TCACCTTGATCTGGTCAGTGGCAAAGGAGCG	M5t22e	GTATTAAACGGGACTAAACAACGTGAAACGTTA
M1t24h	TAATAAAAGGGACATTCTGCCACTAAAGCA	M5t24h	CGTGGCACAGACAATATTTGAGGCAGGTCA
M3t0g	TCGTCACCAGTACAAACTACAACGCTCAGTAC	M7t0g	CACCAACCTCATTTCAGGGATAATCACCGT
M3t2f	CAGCGGAGAACCTATTCTGGTCAGACG	M7t2f	ACTCAGGAACGGGTCAGTGCCTGCAGTC
M3t2e	CTATTCTGTAAGTGCCTCGAGAACTGAGTT	M7t2e	AAGTTTAGGTTAGTACCGCCACTCAGAGC
M3t4f	ATTGGCCTCTCAGAGCCACCACCAATGAAAC	M7t4f	TGAATTACCGGAACCAGAGCCACAGACTGT
M3t4e	CCGCCACCTGATATTCAACACAAACCCCTGC	M7t4e	CAAAATCACCGTTCCAGTAAGCGCTGGTAAT
M3t6f	CATCGATAGACTTGAGCCATTGGAAACGTAG	M7t6f	AGCGCGTTGAGGGAGGGAAAGGTTAAGTTA
M3t6e	CCGTCACCGCAGCACCGTAATCACCTCAGAA	M7t6e	CAACCGATTTCATCGCATTTCGTTCATATA
M3t8f	AAAATACACCGAGGAACGCAAAGGGAGC	M7t8f	TTTTGTCATATCTACCGAAGCCCCGCTAATA
M3t8e	AGAAGGAATACATAAGGTGGCAAATTATCA	M7t8e	GCAATAGCCAATCAATAGAAAATGCGACATT
M3t10f	GCATTAGAAATCCAATAAGAAAATATAGAA	M7t10f	TCAGAGAGACGAGCTCTTCCAGGAGGTT
M3t10e	TTTATCCCCGGGAGAATTAACTGAAGTTACC	M7t10e	CAACGCTAATAACCCACAAGAATATGAAATA
M3t12f	GGCTTATCGCACTCATCGAGAACCCGACAA	M7t12f	TGAAGCTAACCAATCAATAATCAGAACGCG
M3t12e	CAAGTACCCGGTATTCTAAGAACGCCATATTA	M7t12e	CATGTAGATAAAATCAAGATTAGTTAATCTTAC
M3t14f	AGGTAAGGAATGCCATTAAAGAAAAC	M7t14f	CCTGTTATCATATGCGTTACATACACCGAC
M3t14e	TTAATTGATAATTCTGTCAGACTATTAAAC	M7t14e	GTTTAGTATCAACAATAGATAAGTTACGAG
M3t16f	TTTCAAATTAAACCTCCGGTTATTAAACAT	M7t16f	CGTGTGATTAAGACGCTGAGAAGTGAATAAC
M3t16e	CTACTTTATATTAGTTAAATTAGTAGGGC	M7t16e	AGCTTAGAAAATAAGCGTTAAAAAGCCT
M3t18f	TTCATTTGGAGGCGAATTATTCTGATTGTT	M7t18f	CTTGCTTCCATCGGAGAAACAATGCGCTA
M3t18e	ATCGCGCAAATTACCTTTTAACGAGAGA	M7t18e	ACCTTTATGTAATCGCTAACAGCGAT
M3t20f	TGGATTATACAAAGAAACCCAGAACAA	M7t20f	AAACAGAATTAAACCTTGCCTAACAGATT
M3t20e	TTTGCAGAACCTCTGAAATAATGGTTACAA	M7t20e	AACTCGTAATAAGAAATTGCGTAGTAACAGT
M3t22f	GTTGAAAGCAGCAAATGAAAATACAGAGAT	M7t22f	AGAGCGTATAAAACAGAGGTGAATGGCTAT
M3t22e	AGAGCCAGGAATTGAGGAAGGTTATTATCAT	M7t22e	AGCAGAACGAAATAGATAATACATAATTGAC
M3t24h	AGAACCTTCTGACCTGAAAGCGCCACGCTG	M7t24h	TAGTCTTAATGCGCGAACTGATAGAACACC

M-1t0g	CGATCTAAAGTTTGTCTCTTTCGCCG	M-5t0g	AAACAACCTTCAACAGTTCAGCAATTGTAT
M-1t2f	ACAATGACGGTCGCTGAGGCTTCGATTATA	M-5t2f	CGGTTTATAAAGACAGCATCGGAAGGGCACCA
M-1t2e	GATATATTAACAACCACGCCAACAGAGAA	M-5t2e	CAGCAGCGCAGCTGCTTCGAGATTTGCT
M-1t4f	CCAAGCGCCCTGATAATTGTCGCCCTGACG	M-5t4f	ACCTAAAAGACGGTCAATCATAAAGAACCGG
M-1t4e	GTATCATCGAACAAAGTACAACCGCCGCCA	M-5t4e	GAGGCGCACGAAAGAGGCAAAAGGTGACCCCT
M-1t6f	AGAAACACTTAAATTCAACTTACCTCGTT	M-5t6f	ATATTTCATCAGTCAGGACGTTGGTAATGCAG
M-1t6e	TGAGATGGCAGAACGAGTAGTAAACATTACCA	M-5t6e	CATTATACTACCCAAATCAACGTAGCCGGAAC
M-1t8f	ACCAGACGGCAAAAGAAGTTTGTTTAATT	M-5t8f	ATACATAAGCGGAATCGTCATAACAGAACGA
M-1t8e	AGGCTTTACGATAAAAACCAAAATTAAAGAC	M-5t8e	CCAATACTCGCCAAAGGAATTAAACTGGCT
M-1t10f	CGAGCTTCAGGTAGGATTAGAGGTATATT	M-5t10f	AAGCGGATCTTAGAGCTTAATTGGCGAACGA
M-1t10e	ACTCCAACAAAGCGAACCAAGACCGCAGCCTT	M-5t10e	GC GGATGGTGCATAAAAAGATTAGATAGCGT
M-1t12f	TTCATTGACTAATAGTAGTACGAGAGAAAGG	M-5t12f	GTAGATTAGCAATAAGCCTCATAGAACCC
M-1t12e	TCAATTCTGGGCGCAGCTGAAATCATTACC	M-5t12e	CAAAATTAAGTTGACCATTAGATCATTTT
M-1t14f	CCGGAGACGTTCTAGCTGATAAATTAAATT	M-5t14f	TCATATATCAGGTACATGCCTGAACAGGAAG
M-1t14e	ATTCAACCAGTCAAATCACCATTTTCGAG	M-5t14e	AAGGCTATTAAATGCAATGCCTAGAATTAG
M-1t16f	TTGTTAACAAAAATAATTGCGTGCCGAA	M-5t16f	ATTGTATATAACAAACCGTCGGATGACGACGA
M-1t16e	AAAGCCATTAGCTCATTTTTAAATGCAAAT	M-5t16e	TGAGCGAGAGCAAATATTAAATGATCTACA
M-1t18f	ACCAGGCAGTTGGGAGGGCGATCTCACAAAT	M-5t18f	CAGTATCGGCTGCAAGGCATTAGGGTACCG
M-1t18e	GCGCAACTAAGGCCATTGCCAACAAACAA	M-5t18e	GGGGATGTGCCTCAGGAAGATCGATTAAATG
M-1t20f	TCCACACATGGGTGCTTAATGATGCCAG	M-5t20f	AGCTCGAAGTCGGAAACCTGTCGACAGCTGA
M-1t20e	GTAAAGGCCACATACGAGCCGGAAGATCAGATG	M-5t20e	GCTTCCATTGTAATCATGGTCGGCGAAAG
M-1t22f	CAGGC GAAAAAATCCCTTATAAATAGCGGT	M-5t22f	TTGCCCTTAAGAGTCCACTATTAGAACGTGG
M-1t22e	AAATCGGCAATCCTGTTGATGGCAAACCC	M-5t22e	TTTGAACCACCGCCTGGCCCTGCACTGCC
M-1t24h	ACGCTGCGCTAACACCACACCCACGACCAG	M-5t24h	CGAGAAAGGAAGGGAAGAAAGCGTGTCCAG
M-3t0g	TAGTAAATGAATTCTGTATGGGTGAATT	M-7t0g	AATAGAAAGGAACAACAAAGGACTCCAAA
M-3t2f	CTTAAACACGCTTTGCGGGATCAAACACT	M-7t2f	AAAAGGCTTACAGAGGCTTGAGTAAACGGG
M-3t2e	TTAAAGGCCTTGTACCGATAGCCAGACGT	M-7t2e	GCAACGGCCAAAAGGAGCCTTGAGTGAG
M-3t4f	AAAACACTGCTCCATGTTACTTAACAAAGCT	M-7t4f	TAAAATACAACTTGAAAGAGGACTGGCTGAC
M-3t4e	CGCGACCTCATTTGACCCCCAGGCAGGGAG	M-7t4e	AACTGACCGTAATGCCACTACGACGGAGGGTA
M-3t6f	GCTCATTCTATGCGATTAAAGCAGGGCAT	M-7t6f	CTTCATCATAATAAACGAACTAATCAGTTG
M-3t6e	GAATTACCACTGAAATAAGGCTTGTGCGAACATC	M-7t6e	ATCTACGTAGAGTAATCTGACAGGAAACCG
M-3t8f	AGTAAGAGTAAATGTTAGACTGAGAGGAAG	M-7t8f	AGATTAGCCTCAAATGCTTAAAAATCAG
M-3t8e	GGTAATAGCAACACTATCATAACATCATTG	M-7t8e	TGAATCCGAATACCACTTCAACGAAGAAAA
M-3t10f	CCCGAAAGCCTTTGATAAGAGGTACATTTC	M-7t10f	GTCTTACAGCTCAACATGTTTATCATTCA
M-3t10e	TAATTGCTACTCAAATATCGGCCAGAGGG	M-7t10e	AATGCTGTCCTGACTATTATAGTATATTCA
M-3t12f	GCAAATGGCATACAGGCAAGGCAAGAGTAATG	M-7t12f	TATAACAGCGGTGTACCAAAAAGCCTTAT
M-3t12e	CAATAAATTCAATAACCTGTTAACGTACCTT	M-7t12e	AGCTAAATTGATTCCAATTCTCTGAATAT
M-3t14f	TGTAGGTATAGCTATTGAGATGTAACAG	M-7t14f	TTCAACGCAGAGAATCGATGAAACGACCCGGT
M-3t14e	GGAGAGGGAGATTCAAAAGGTTAACATC	M-7t14e	AGCAAACAAAGATAAAAATTGAGCATAA
M-3t16f	TTAATATTCCAGCTTCATCAACCACTCCAG	M-7t16f	TGATAATCCGGCGATTGACCGTCATCGTAA
M-3t16e	TCCTGTAGTTGTTAAAATCGCATTATGCC	M-7t16e	GGAACAAAAGAAAAGCCCCAAAAGAGTCTGG
M-3t18f	CCAGCTTGCTATTAGCCAGCTATAGCTGT	M-7t18f	CCGTGCATGGTTTCCCAGTCACGATGCC
M-3t18e	GCCTCTCCCGGACCGCTTCTGGTCTGGCCT	M-7t18e	AACGCCAGCTGCCAGTTGAGGGTCTCCGTG
M-3t20f	TTCTGTGTAATTGCGTTCGCTAGAGAGTT	M-7t20f	CAGGTCGAGAACGCCAACGCCGGGGTT
M-3t20e	ACTCACATTGAAATTGTTATCGCGGTGCGG	M-7t20e	GCATTAATCTCTAGAGGATCCCCAGTTGGGT
M-3t22f	GCAGCAAGAGATAGGGTTGAGTGTAAAGGAGC	M-7t22f	TTCTTTCACGTCAAAGGGCGAACCCGATTT
M-3t22e	ATAGCCCGGGTCCACGCTGGTTGTGAGCTA	M-7t22e	GGACTCCAACCAAGTGGACGGGATGCCAGCT
M-3t24h	GGCGCTAGGGCGCTGGCAAGTGTCAAAAGA	M-7t24h	AGAGCTTGACGGGGAAAGCCGGCAAGAACGT

M9t0i	TTTCCTCAGAACGCCACCCCTCAGA
M9t2f	ACCGCCACTTTATGATACAGGAGTGTATCATACAT
M9t4f	GGCTTTGTTTAGCGTTGCCATCTGTCATAGC
M9t6f	CCCCTTATTTGCCAAAGACAAAAGGTATATGG
M9t8f	TTTACCAAGTTTATAAGAGCAAGAACATGAGTTAA
M9t10f	GCCCAATATTTCTACATTTATCCTGGCTATTTT
M9t12f	GCACCCAGTTTAATATCCCCTAATCCTGAAC
M9t14f	AAGAAAAATTAACTATAATTACTAGATAAGAATA
M9t16f	AACACCGGTTTAACTGAAATCCTTGAAACTTAATTAA
M9t18f	TTTCCCTTTGTCAGATGAATACAGATTTCA
M9t20f	GGTTTAACTTTATTAGACTTACAAACTTGAGGAT
M9t22j	TTAGAAGTTTATTAAAAATACCGAACGCCCTAAACATGCCCTTT
M-9t2i	ACTTTTCTTTTCACGTTGAAATATTGCGAATAATAATT
M-9t4e	GGTGTACATTTATGAGGAAGTTCCATGACTAAAG
M-9t6e	ACATTATTTGACCAGGCGCATAGGCAGATGAAAC
M-9t8e	GAAAACGATTTACAGGTAGAAAGATTACGGAAACA
M-9t10e	ACTAAAGTTTGAATGACCATAATCACAGTTCA
M-9t12e	CCCTGTAATTTACGGTGTCTGAAAGTTAATATGCA
M-9t14e	AAAACTAGTTTACTTTGCGGGAGAACATTATGA
M-9t16e	AGGTCACGTTTCATGTCATATGTGAATCGT
M-9t18e	AAACGACGTTTTGGGTAGATGGCGAATGGGAT
M-9t20e	GGCGGTTTTGCCAGTGCAGCTTGACGTTGTA
M-9t22e	TATCACGGTTTGCATGGCGCCAGCGGGAGA
M-9t24j	TTTAACCTAAAGGGAGCCAAACCGTC
Mem1	TATTACATTGGCAGATTCAACAGTCAC
Mem2	TTTGACGCTCAATCGCTGAAATGGAT
Mem3	AGGAAAAACGCTCATGAAATACCTACA
Mem4	AACAATATTACGCCAGCCATTGCAAC
Mem5	ACTATCGCCCTGCTGGTAATATCCAG
Mem6	ATCACTGCGCTGAGTAGAAGAACTCAA
Mem7	AGCAATACTTCTTGATTAGTAATAAC
Mem8	GCCCGCCTTAATGCCCGCTACAGGGC
Mem9	GCGTACTATGGTGCTTGACGAGCAC
Mem10	GTATAACGTGCTTCCTCGTTAGAATC
Mem11	AGAGCGGGAGCTAACAGGAGGCCAT
Mem12	TAAAGGGATTTAGACAGGAACGGTAC
Mem13	GCCAGAACCTGAGAAGTGTGTTTATA
Mem14	ATCAGTGAGGCCACCGAGTAAAGAGT
Mem15	CTGTCCATCACGCAAATTAAACCGTTGT

**Supplementary Table 2.** Unmodified staple strands for Tile type B (Supplementary Figure 2), used in fluorescence experiments.

#### 4. Supplementary Movie Legends.

**Supplementary Movie 1.** Sequence of high-speed AFM images, corresponding to the data shown in Figure 4, showing a motor strand moving through two discrete transitions between stators. Periods of rapid movement between adjacent stators are followed by slower transitions in which the motor advances a single step. The kymograph (Fig. 4) is shown beside the movie, and the fitted motor position is plotted on the kymograph as the movie plays. Blue lines indicate inferred stator positions. Images were obtained at 23°C in a buffer containing 10 mM Tris-HCl (pH 7.6), 1 mM EDTA, and 10 mM MgCl<sub>2</sub> after treatment with nicking enzyme Nt.BbvCI. Images were recorded at 0.1 fps, play back is at 50× (5 fps).

**Supplementary Movie 2.** High-speed AFM images of a motor strand moving between two adjacent stators, corresponding to the kymograph shown in Supplementary Fig. 12. Periods of rapid movement between adjacent stators are attributed to branch migration of the motor (Figure 1). Images were obtained at 23°C in a buffer containing 10 mM Tris-HCl (pH 7.6), 1 mM EDTA, and 10 mM MgCl<sub>2</sub> after treatment with nicking enzyme Nt.BbvCI. Images were recorded at 0.2 fps, play back is at 25× (5 fps).

## 5. Supplementary Notes.

- (1) Rothemund, P. W. K. Folding DNA to create nanoscale shapes and patterns. *Nature* **440**, 297-302 (2006).
- (2) Dietz, H., Douglas, S. M. & Shih, W. M. Folding DNA into Twisted and Curved Nanoscale Shapes. *Science* **325**, 725-730 (2009).
- (3) Abramoff, M.D., Magelhaes, P. J., & Ram, S. J. Image Processing with ImageJ. *Biophotonics International*, **11**, 36-42 (2004).
- (4) Bath, J., Green, S. J. & Turberfield, A. J. A free-running DNA motor powered by a nicking enzyme. *Angew. Chem. Int. Edn.* **44**, 4358-4361 (2005).